ELSEVIER

Contents lists available at ScienceDirect

Computers & Fluids

journal homepage: www.elsevier.com/locate/compfluid



Technical note

Absorbing boundary condition for nonlinear Euler equations in primitive variables based on the Perfectly Matched Layer technique

D.K. Lin^a, X.D. Li^{a,*}, Fang Q. Hu^b

- ^a School of Jet Propulsion, Beihang University, Beijing 100191, People's Republic of China
- ^b Department of Mathematics and Statistics, Old Dominion University, Norfolk, VA 23529, United States

ARTICLE INFO

Article history: Received 31 January 2010 Received in revised form 12 July 2010 Accepted 23 August 2010 Available online 27 August 2010

Keywords:
Nonreflecting boundary condition
Perfectly Matched Layer
Nonlinear Euler equations
Primitive variables
Computational Aeroacoustics

ABSTRACT

For aeroacoustics problems, the nonlinear Euler equations are often written in primitive variables in which the pressure is treated as a solution variable. In this paper, absorbing boundary conditions based on the Perfectly Matched Layer (PML) technique are presented for nonlinear Euler equations in primitive variables. A pseudo mean flow is introduced in the derivation of the PML equations for increased efficiency. Absorbing equations are presented in unsplit physical primitive variables in both the Cartesian and cylindrical coordinates. Numerical examples show the effectiveness of the proposed equations although they are not theoretically perfectly matched to the nonlinear Euler equations. The derived equations are tested in numerical examples and compared with the PML absorbing boundary condition in conservation form that was formulated in an earlier work. The performance of the PML in primitive variables is found to be close to that of the conservation formulation. A comparison with the linear PML in nonlinear problems is also considered. It is found that using nonlinear absorbing equations presented in this paper significantly improves the performance of the absorbing boundary condition for strong nonlinear cases.

© 2010 Elsevier Ltd. All rights reserved.

1. Introduction

Perfectly Matched Layer (PML) is a technique of developing non-reflecting boundary conditions. Similar to the buffer zone and sponge layer techniques [1,2], extra absorbing zones are added, in which numerical solutions are damped [3]. However, PML zones are usually much thinner compared to most other buffer zones, as the absorbing zone is theoretically reflectionless for multi-dimensional linear waves of any angle and frequency. Berenger proposed firstly the PML for Maxwell's equations to absorb the electromagnetic wave at open boundaries in 1994 [4]. Berenger's technique was first applied to the linear Euler equations with a uniform mean flow for the field of acoustics in 1996 [5]. Since then, many efforts have been made in the study of the PML technique and to extend its application and improve its performance. Some recent advances in the development of PML as absorbing boundary conditions were reviewed in Ref. [3]. In recent years, many progresses have been made in the development of PML for Computational Fluid Dynamics (CFD) and Computational Aeroacoustics (CAA). It started with the cases for the linearized Euler equations from constant mean flows to non-uniform mean flows [5-11], then extended to the cases for the fully nonlinear Euler equations [12].

E-mail addresses: lixd@buaa.edu.cn (X.D. Li), fhu@odu.edu (F.Q. Hu).

And the applications of PML to linearized Navier–Stokes equations [13] and nonlinear Navier–Stokes equations [14] have been discussed. Recently, PML for the fully nonlinear Euler and Navier–Stokes equations has been given in Ref. [15]. And in addition, PML equations were developed to accommodate the uniform mean flow in an arbitrary direction [16].

In our previous study of PML for nonlinear problems, the Euler and Navier-Stokes equations were given in the conservation form [15]. In the present paper, a PML absorbing boundary condition for the nonlinear Euler equations in primitive variables is developed. This is motivated by the observation that the nonlinear Euler equations in primitive variables remain a popular form of the governing equations for inviscid compressible flows, especially for many nonlinear aeroacoustics problems. The purpose of this paper is two-fold. First, new absorbing boundary conditions in primitive variables based on the PML technique are proposed for both the Cartesian and cylindrical coordinate systems. Second, comparisons in the performance with the nonlinear PML in the conservation form and the linear PML in primitive variables are conducted, to demonstrate the accuracy and necessity of proposed new set of boundary conditions. To deal with the nonlinear terms involving spatial derivatives and to facilitate the application of PML complex change of variables in frequency domain, new auxiliary variables are introduced. The final form of the absorbing equations is presented in unsplit physical primitive variables. Numerical examples

^{*} Corresponding author.

are presented to demonstrate the validity and efficiency of the proposed boundary conditions. In the next section, PML equations for the nonlinear Euler equations in primitive variables are derived. It follows a three-step method proposed in Refs. [10,15]. Firstly, a proper space-time transformation is applied to the governing equations, so that linear waves have consistent phase and group velocities. Secondly, a PML complex change of variables is applied in the frequency domain. And thirdly, the time domain PML absorbing boundary condition is derived by a conversion of the frequency domain equations to the time domain equations. Numerical examples that validate the efficiency and validity of the proposed PML equations are presented in Section 3. Concluding remarks are given in Section 4.

2. PML equations in primitive variables

2.1. Cartesian coordinates

The two-dimensional nonlinear Euler equations in primitive variables are written in the Cartesian coordinate system as

$$\frac{\partial \mathbf{u}}{\partial t} + \mathbf{A} \frac{\partial \mathbf{u}}{\partial x} + \mathbf{B} \frac{\partial \mathbf{u}}{\partial y} = 0 \tag{1}$$

$$\mathbf{u} = \begin{bmatrix} \rho \\ u \\ v \\ p \end{bmatrix}, \quad \mathbf{A} = \begin{bmatrix} u & \rho & 0 & 0 \\ 0 & u & 0 & 1/\rho \\ 0 & 0 & u & 0 \\ 0 & \gamma p & 0 & u \end{bmatrix}, \quad \mathbf{B} = \begin{bmatrix} v & 0 & \rho & 0 \\ 0 & v & 0 & 0 \\ 0 & 0 & v & 1/\rho \\ 0 & 0 & \gamma p & v \end{bmatrix}$$

where u and v are the velocity components in x and y directions, respectively, p is the pressure, ρ is the density. In this paper, the velocity is nondimensionalized by a reference speed of sound c_{∞} , density by a reference density ρ_{∞} and pressure by $\rho_{\infty}c_{\infty}^2$.

We wish to formulate absorbing equations so that out-going disturbances can be exponentially reduced once they enter a PML domain while causing as little numerical reflection as possible. For nonlinear Euler equations, the solutions can often be partitioned into two parts. One part is the time-independent mean state, the other part is the time-dependent fluctuation. It would be efficient to absorb only the time-dependent fluctuations in the PML domains. When the mean flow is unknown, an approximate mean flow or a pseudo mean flow can be used in the formulation as in Ref. [17]. Therefore, we express the primitive variables inside a PML domain as

$$\mathbf{u} = \bar{\mathbf{u}} + \mathbf{u}' \tag{2}$$

where the superscript "bar" indicates the mean flow (or the pseudo mean flow), and the superscript "prime" indicates the difference between the mean flow and the actual flow. The mean flow or pseudo mean flow should satisfy the steady Euler equations,

$$\overline{A}\frac{\partial \overline{u}}{\partial x} + \overline{B}\frac{\partial \overline{u}}{\partial y} = 0 \tag{3}$$

According to Eqs. (1)–(3), we can get the following equation for the time dependent part of the solution:

$$\frac{\partial \mathbf{u}'}{\partial t} + \mathbf{A} \frac{\partial \mathbf{u}}{\partial x} + \mathbf{B} \frac{\partial \mathbf{u}}{\partial y} - \overline{\mathbf{A}} \frac{\partial \overline{\mathbf{u}}}{\partial x} - \overline{\mathbf{B}} \frac{\partial \overline{\mathbf{u}}}{\partial y} = 0$$
 (4)

We shall derive absorbing equations for Eq. (4). To facilitate the derivation, Eq. (4) can be rewritten as

$$\begin{split} \frac{\partial u'}{\partial t} + \overline{A} \frac{\partial (u - \overline{u})}{\partial x} + (A - \overline{A}) \frac{\partial \overline{u}}{\partial x} + (A - \overline{A}) \frac{\partial (u - \overline{u})}{\partial x} + \overline{B} \frac{\partial (u - \overline{u})}{\partial y} \\ + (B - \overline{B}) \frac{\partial \overline{u}}{\partial y} + (B - \overline{B}) \frac{\partial (u - \overline{u})}{\partial y} &= 0 \end{split} \tag{5}$$

For the stability of the PML, a space-time transformation $\bar{t} = t + \beta x$ is necessary in the derivation process, where β is a parameter dependent on the mean flow profile, as discussed in Refs. [10,15]. Here, a mean flow that is dominantly in the x direction is assumed. In transformed coordinates, Eq. (5) can be written as follows:

$$\begin{split} \frac{\partial \mathbf{u}'}{\partial \bar{t}} + \beta \overline{\mathbf{A}} \frac{\partial (\mathbf{u} - \bar{\mathbf{u}})}{\partial \bar{t}} + \beta (\mathbf{A} - \overline{\mathbf{A}}) \frac{\partial (\mathbf{u} - \bar{\mathbf{u}})}{\partial \bar{t}} + \overline{\mathbf{A}} \frac{\partial (\mathbf{u} - \bar{\mathbf{u}})}{\partial x} \\ + (\mathbf{A} - \overline{\mathbf{A}}) \frac{\partial (\mathbf{u} - \bar{\mathbf{u}})}{\partial x} + (\mathbf{A} - \overline{\mathbf{A}}) \frac{\partial \bar{\mathbf{u}}}{\partial x} + \overline{\mathbf{B}} \frac{\partial (\mathbf{u} - \bar{\mathbf{u}})}{\partial y} + (\mathbf{B} - \overline{\mathbf{B}}) \frac{\partial (\mathbf{u} - \bar{\mathbf{u}})}{\partial y} \\ + (\mathbf{B} - \overline{\mathbf{B}}) \frac{\partial \bar{\mathbf{u}}}{\partial y} = 0 \end{split} \tag{6}$$

In the frequency domain, we have

$$(-i\omega)\widetilde{\mathbf{u}}' + (-i\omega)\beta\overline{\mathbf{A}}(\widetilde{\mathbf{u}} - \widetilde{\mathbf{u}}) + \beta(\widetilde{\mathbf{A}} - \widetilde{\mathbf{A}}) * (-i\omega)(\widetilde{\mathbf{u}} - \widetilde{\mathbf{u}})$$

$$+ \overline{\mathbf{A}}\frac{\partial(\widetilde{\mathbf{u}} - \widetilde{\mathbf{u}})}{\partial x} + (\widetilde{\mathbf{A}} - \overline{\mathbf{A}}) * \frac{\partial(\widetilde{\mathbf{u}} - \widetilde{\mathbf{u}})}{\partial x} + (\widetilde{\mathbf{A}} - \overline{\mathbf{A}})\frac{\partial \overline{\mathbf{u}}}{\partial x}$$

$$+ \overline{\mathbf{B}}\frac{\partial(\widetilde{\mathbf{u}} - \widetilde{\mathbf{u}})}{\partial y} + (\widetilde{\mathbf{B}} - \overline{\mathbf{B}}) * \frac{\partial(\widetilde{\mathbf{u}} - \widetilde{\mathbf{u}})}{\partial y} + (\widetilde{\mathbf{B}} - \overline{\mathbf{B}})\frac{\partial \overline{\mathbf{u}}}{\partial y} = 0$$

$$(7)$$

where a tilde indicates the time Fourier transformed variable and * denotes convolution integral.

By applying the PML complex change of variables to Eq. (7), we

$$\begin{split} (-i\omega)\widetilde{\mathbf{u}}' + (-i\omega)\beta\overline{\mathbf{A}}(\widetilde{\mathbf{u}} - \widetilde{\mathbf{u}}) + \beta(\widetilde{\mathbf{A}} - \widetilde{\mathbf{A}}) &* (-i\omega)(\widetilde{\mathbf{u}} - \widetilde{\mathbf{u}}) \\ + \overline{\mathbf{A}}\frac{\partial(\widetilde{\mathbf{u}} - \widetilde{\mathbf{u}})}{\partial x} \frac{1}{1 + \frac{i\sigma_x}{\omega}} + (\widetilde{\mathbf{A}} - \overline{\mathbf{A}}) &* \frac{\partial(\widetilde{\mathbf{u}} - \widetilde{\mathbf{u}})}{\partial x} \frac{1}{1 + \frac{i\sigma_x}{\omega}} \\ + (\widetilde{\mathbf{A}} - \overline{\mathbf{A}})\frac{\partial\overline{\mathbf{u}}}{\partial x} + \overline{\mathbf{B}}\frac{\partial(\widetilde{\mathbf{u}} - \widetilde{\mathbf{u}})}{\partial y} \frac{1}{1 + \frac{i\sigma_y}{\omega}} \\ + (\widetilde{\mathbf{B}} - \overline{\mathbf{B}}) &* \frac{\partial(\widetilde{\mathbf{u}} - \widetilde{\mathbf{u}})}{\partial y} \frac{1}{1 + \frac{i\sigma_y}{\omega}} + (\widetilde{\mathbf{B}} - \overline{\mathbf{B}})\frac{\partial\overline{\mathbf{u}}}{\partial y} = 0 \end{split} \tag{8}$$

where σ_x and σ_y are absorption coefficients, which are positive and could be functions of x and y, respectively [5].

To rewrite the above equation in the time domain, we introduce auxiliary variables \mathbf{q}_1 and \mathbf{q}_2 as

$$(-i\omega)\tilde{\mathbf{q}}_{1} = \frac{\partial (\widetilde{\mathbf{u} - \bar{\mathbf{u}}})}{\partial x} \frac{1}{1 + \frac{i\sigma_{x}}{\omega}} + (-i\omega)\beta(\widetilde{\mathbf{u} - \bar{\mathbf{u}}})$$
(9)

$$(-i\omega)\tilde{\mathbf{q}}_2 = \frac{\partial (\widetilde{\mathbf{u} - \widetilde{\mathbf{u}}})}{\partial y} \frac{1}{1 + \frac{i\sigma_y}{\omega}}$$
(10)

Then Eq. (8) becomes

$$\begin{split} (-i\omega)\widetilde{\mathbf{u}}' + \overline{\mathbf{A}}(-i\omega)\widetilde{\mathbf{q}}_1 + (\widetilde{\mathbf{A}} - \overline{\mathbf{A}}) \ * \ (-i\omega)\widetilde{\mathbf{q}}_1 + \overline{\mathbf{B}}(-i\omega)\widetilde{\mathbf{q}}_2 \\ + (\widetilde{\mathbf{B}} - \overline{\mathbf{B}}) \ * \ (-i\omega)\widetilde{\mathbf{q}}_2 + (\widetilde{\mathbf{A}} - \overline{\mathbf{A}})\frac{\partial \overline{\mathbf{u}}}{\partial x} + (\widetilde{\mathbf{B}} - \overline{\mathbf{B}})\frac{\partial \overline{\mathbf{u}}}{\partial y} &= 0 \end{split} \tag{11}$$

It is easy to get the time domain equations for \mathbf{q}_1 and \mathbf{q}_2 in the original space-time domain as

$$\frac{\partial \mathbf{q}_{1}}{\partial t} + \sigma_{x} \mathbf{q}_{1} = \frac{\partial (\mathbf{u} - \bar{\mathbf{u}})}{\partial x} + \sigma_{x} \beta (\mathbf{u} - \bar{\mathbf{u}})$$

$$\frac{\partial \mathbf{q}_{2}}{\partial t} + \sigma_{y} \mathbf{q}_{2} = \frac{\partial (\mathbf{u} - \bar{\mathbf{u}})}{\partial y}$$
(12)

$$\frac{\partial \mathbf{q}_2}{\partial t} + \sigma_y \mathbf{q}_2 = \frac{\partial (\mathbf{u} - \bar{\mathbf{u}})}{\partial v} \tag{13}$$

Rewriting Eq. (11) back into the original space-time domain, we get

$$\begin{split} \frac{\partial \mathbf{u}'}{\partial t} + \overline{\mathbf{A}} \frac{\partial \mathbf{q}_1}{\partial t} + (\mathbf{A} - \overline{\mathbf{A}}) \frac{\partial \mathbf{q}_1}{\partial t} + \overline{\mathbf{B}} \frac{\partial \mathbf{q}_2}{\partial t} + (\mathbf{B} - \overline{\mathbf{B}}) \frac{\partial \mathbf{q}_2}{\partial t} \\ + (\mathbf{A} - \overline{\mathbf{A}}) \frac{\partial \overline{\mathbf{u}}}{\partial x} + (\mathbf{B} - \overline{\mathbf{B}}) \frac{\partial \overline{\mathbf{u}}}{\partial y} &= 0 \end{split} \tag{14}$$

Finally, using Eqs. (12)–(14) can be written as

$$\frac{\partial \mathbf{u}}{\partial t} + \mathbf{A} \frac{\partial \mathbf{u}}{\partial x} + \mathbf{B} \frac{\partial \mathbf{u}}{\partial y} - \overline{\mathbf{A}} \frac{\partial \overline{\mathbf{u}}}{\partial x} - \overline{\mathbf{B}} \frac{\partial \overline{\mathbf{u}}}{\partial y} + \sigma_x \beta \mathbf{A} (\mathbf{u} - \overline{\mathbf{u}}) - \sigma_x \mathbf{A} \mathbf{q}_1 - \sigma_y \mathbf{B} \mathbf{q}_2 = 0$$
(15)

Eqs. (12), (13) and (15) form the absorbing equations for nonlinear Euler equations in primitive variables to be used in the PML domain.

2.2. Cylindrical coordinates

The three-dimensional nonlinear Euler equations in primitive variables are expressed in the cylindrical coordinate system as

$$\frac{\partial \mathbf{u}}{\partial t} + \mathbf{A} \frac{\partial \mathbf{u}}{\partial z} + \mathbf{B} \frac{\partial \mathbf{u}}{\partial r} + \frac{1}{r} \mathbf{C} \mathbf{u} + \frac{1}{r} \mathbf{D} \frac{\partial \mathbf{u}}{\partial \theta} = 0$$
 (16)

where

$$\mathbf{u} = \begin{bmatrix} \rho \\ v_z \\ v_r \\ v_\theta \\ p \end{bmatrix}, \ \ \mathbf{A} = \begin{bmatrix} v_z & \rho & 0 & 0 & 0 \\ 0 & v_z & 0 & 0 & 1/\rho \\ 0 & 0 & v_z & 0 & 0 \\ 0 & 0 & v_z & 0 & 0 \\ 0 & \gamma p & 0 & 0 & v_z \end{bmatrix}, \ \ \mathbf{B} = \begin{bmatrix} v_r & 0 & \rho & 0 & 0 \\ 0 & v_r & 0 & 0 & 0 \\ 0 & 0 & v_r & 0 & 1/\rho \\ 0 & 0 & 0 & v_r & 0 \\ 0 & 0 & \gamma p & 0 & v_r \end{bmatrix},$$

where ρ is the density, v_r , v_θ and v_z are velocity components in the radial r, circumferential θ and axial z directions, respectively, and p is the pressure.

Following similar steps given in Section 2.1 for the cartesian coordinates, PML equations in the cylindrical coordinate can be written as

$$\begin{split} \frac{\partial \mathbf{u}}{\partial t} + \mathbf{A} \frac{\partial \mathbf{u}}{\partial z} + \mathbf{B} \frac{\partial \mathbf{u}}{\partial r} + \frac{1}{r} \mathbf{C} \mathbf{u} + \frac{1}{r} \mathbf{D} \frac{\partial \mathbf{u}}{\partial \theta} - \overline{\mathbf{A}} \frac{\partial \overline{\mathbf{u}}}{\partial z} - \overline{\mathbf{B}} \frac{\partial \overline{\mathbf{u}}}{\partial r} - \frac{1}{r} \overline{\mathbf{C}} \overline{\mathbf{u}} \\ - \frac{1}{r} \overline{\mathbf{D}} \frac{\partial \overline{\mathbf{u}}}{\partial \theta} + \sigma_z \beta \mathbf{A} (\mathbf{u} - \overline{\mathbf{u}}) - \sigma_z \mathbf{A} \mathbf{q}_1 - \sigma_r \mathbf{B} \mathbf{q}_2 \\ - \left(\mathbf{C} \mathbf{q}_3 + \mathbf{D} \frac{\partial \mathbf{q}_3}{\partial \theta} \right) \frac{1}{r} \int_{r_0}^{r} \sigma_r dr = 0 \end{split} \tag{17}$$

$$\frac{\partial \mathbf{q}_1}{\partial t} + \sigma_z \mathbf{q}_1 = \frac{\partial (\mathbf{u} - \bar{\mathbf{u}})}{\partial z} + \sigma_z \beta (\mathbf{u} - \bar{\mathbf{u}}) \tag{18}$$

$$\frac{\partial \mathbf{q}_2}{\partial t} + \sigma_r \mathbf{q}_2 = \frac{\partial (\mathbf{u} - \bar{\mathbf{u}})}{\partial r} \tag{19}$$

$$\frac{\partial \mathbf{q}_3}{\partial t} + \frac{\mathbf{q}_3}{r} \int_{r_0}^r \sigma_r dr = \frac{\mathbf{u} - \bar{\mathbf{u}}}{r}$$
 (20)

where r_0 is the interface of Euler and PML domains. σ_z and σ_r are absorption coefficients, which are positive and could be functions of z and r, respectively.

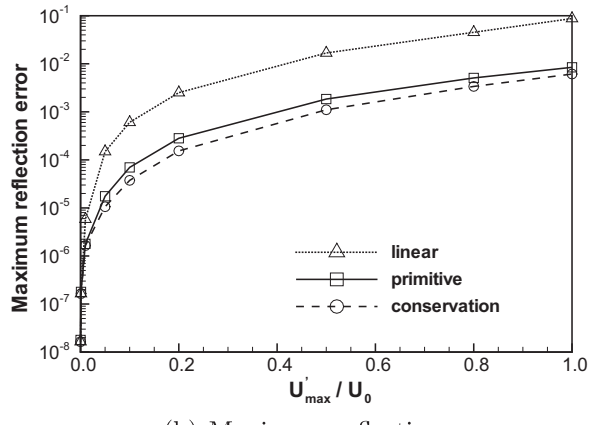
3. Numerical examples

In this section, we present numerical examples of using PML absorbing boundary conditions in primitive variables for nonlinear Euler equations. In all the examples, the Dispersion-Relation-Preserving (DRP) finite difference scheme [18] is applied for spatial discretization and the optimized 2N-storage 5- and 6-stage alternating Low-Dissipation and Low-Dispersion Runge-Kutta (LDDRK) scheme [19] is used for time integration. Numerical examples include an isentropic vortex propagating downstream, a pressure wave propagation and nonlinear acoustic radiation from an oscillating piston in a wall.

3.1. Isentropic vortex

This numerical example is a classical test case for the performance of nonlinear non-reflecting boundary condition [12,15]. A similar calculation has been performed for the PML absorbing boundary condition of the nonlinear Euler equations in conservation form in Ref. [12]. A comparison in the performance of PML equations will be given here.

The details of this case were given in Ref. [12]. Computational domain is $(x,y) \in [-1.4,1.4]$ with $\Delta x = \Delta y = 0.02$. To assess the magnitude of reflection error, Fig. 1(a) plots the maximum reflection error in the v-velocity component relative to the maximum velocity U'_{max} of the vortex along x = 0.9 near the outflow boundary for various strengths of the vortex. The maximum relative reflection error is around 1% with PML width of 20 grid points when the vortex strength $U'_{max} = 0.8U_0$, where U_0 is the background mean velocity. Fig. 1(b) shows the maximum reflection error in a log scale, for the v-velocity component, as a function of the vortex strength U'_{max}/U_0 . It also plots the results calculated by applying the PML equations in the conservation form [15] and the linear PML equations given in Ref. [7]. While the performances of the nonlinear PML equations in the conservation form and in the



(b) Maximum reflection error

Fig. 1. Reflection error (v-velocity component) along x = 0.9 near the outflow boundary for the cases with different vortex strengths U'_{max} . PML width $D = 20\Delta x$.

primitive form are similar, the error caused by using a linear PML is an order of magnitude larger.

3.2. Pressure pulse

In the second example, a strong pressure pulse is introduced into a uniform flow. The propagation of the pressure is simulated by applying the PML absorbing boundary condition for nonlinear Euler equations in primitive variables. The initial condition is $\rho=\rho_0$, $u=U_0$, $v=V_0$ and $p=P_0+P'_{max}e^{-\ln(2)(x^2+y^2)/0.2^2}$, where $\rho_0=1$, $U_0=0.5$, $V_0=0$, $P_0=\frac{1}{\gamma}$ and $P'_{max}=P_0$. The computational domain and mesh are the same as those in the previous example. In both

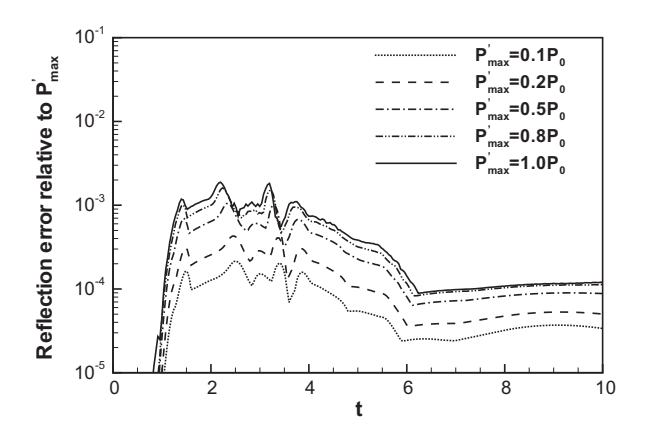


Fig. 2. Maximum relative reflection error (pressure component) along lines $x = \pm 0.9$ and $y = \pm 0.9$ near the PML domain. PML width $D = 20\Delta x$.

examples shown here, the pseudo mean flow is the background uniform flow, i.e. (ρ_0, U_0, V_0, P_0) . Parameter $\beta = U_0/\left(1 - U_0^2\right)$.

Fig. 2 plots the time history of maximum reflection errors for different strengths of the pressure pulse, along lines $x = \pm 0.9$ and $y = \pm 0.9$ close to PML boundaries. Although reflection error increases with the strength of the pressure pulse, the relative error is less than 0.2% for all cases with PML width of 20 grid points.

3.3. Nonlinear acoustic radiation from an oscillating piston

In this example, nonlinear acoustic radiation from an oscillating piston in a wall is simulated. The Euler equations in primitive variables in two-dimensional Cartesian coordinates are solved in the interior domain. The wall is at y=0. The piston is located at $-10 \leqslant x \leqslant 10$, y=0. And velocity of the piston $v=A\sin(\pi t/20)$, where A is a constant. The entire computational domain is $0 \leqslant y \leqslant 110$, $-110 \leqslant x \leqslant 110$ with $\Delta x = \Delta y = 1.0$. Two-dimensional nonlinear PML Eqs. (12), (13) and (15) are solved in PML domains with a width of 10 grid points at the top, left and right boundaries. And parameter β is set based on the mean flow U_0 , i.e., $\beta = U_0/(1-U_0^2)$. Different cases will be simulated, including different velocity amplitudes of the piston A and different incoming flows U_0 . A shock-capturing methodology based on adaptative spatial filtering [20] is used to catch the strong nonlinear phenomenon during the acoustic radiation.

Fig. 3 shows pressure contours at the beginning of a period of piston oscillation for A = 0.2 with different incoming flow U_0 . Dashed lines indicate reference solutions calculated by a large computational domain of $[-600,600] \times [0,600]$. They are in good agreement. Fig. 4 shows the time history of the maximum

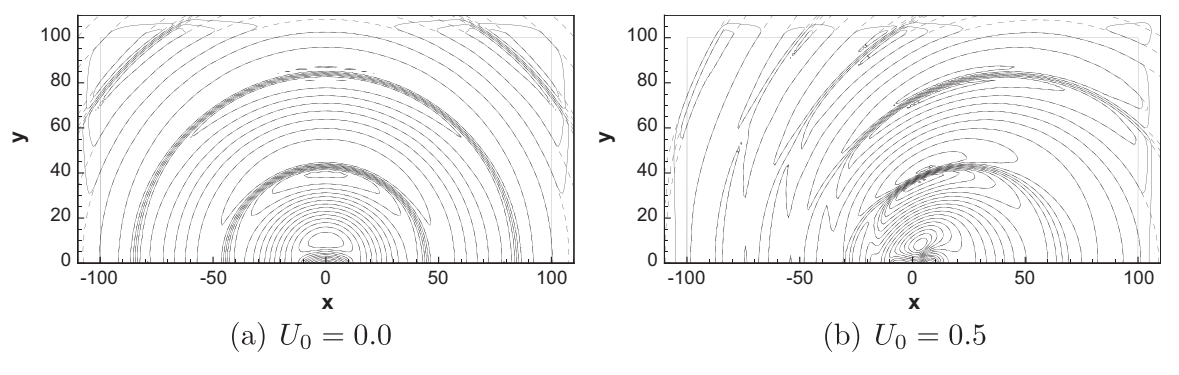


Fig. 3. Pressure contour levels in every 0.02 from 0.5 to 1.0, at the beginning of a cycle. A = 0.2. Solid line: computational; dashed line: large domain calculation.

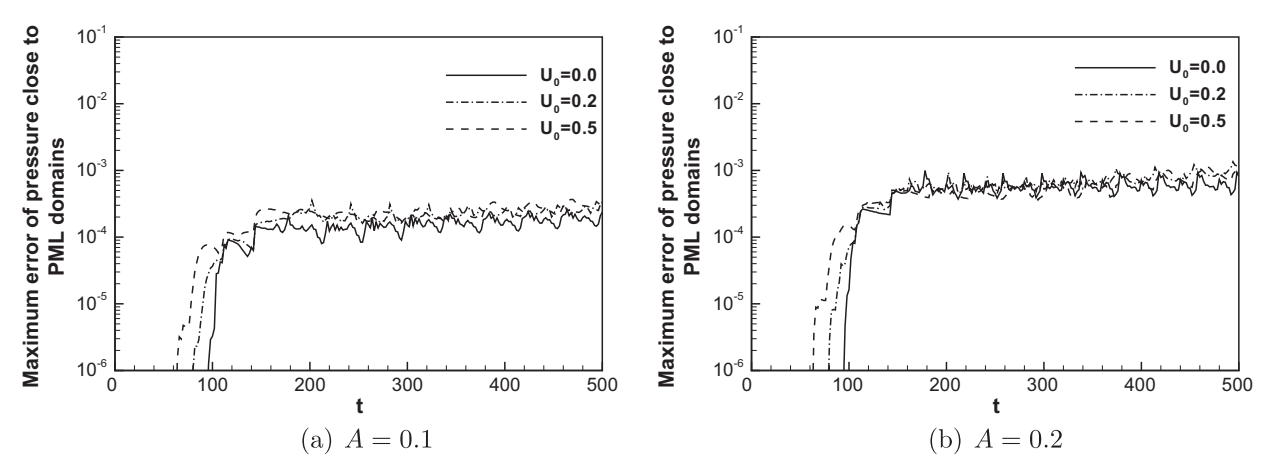


Fig. 4. Maximum reflection error along lines $x = \pm 95$ and y = 95 close to PML domains.

reflection error for the pressure along lines $x = \pm 95$ and y = 95 close to PML domains, from t = 0 to t = 500. The reflection error is obtained by comparing numerical solution with the reference solution.

In addition, acoustic radiation from an oscillating circular piston in a wall is also simulated using equations in Section 2.2 with good results. The details are not given due to limited space.

4. Conclusion

In many aeroacoustics problems, the nonlinear Euler equations are solved using the primitive variables. Although the Perfectly Matched Layer (PML) for the linearized Euler equations was first derived in primitive variables, its direct use in strongly nonlinear problems is not very effective, as demonstrated in this study. In this paper, PML absorbing boundary conditions for nonlinear Euler equations in primitive variables have been derived. Two versions of PML equations for nonlinear Euler equations in primitive variables are given. One is in the two-dimensional Cartesian coordinate system, the other is for the 3D nonlinear Euler equations in cylindrical coordinates. Although the nonlinear equations are not theoretically perfectly matched, the stability and effectiveness of the proposed PML as absorbing boundary condition are demonstrated by numerical examples, including absorption of an isentropic vortex, a nonlinear pressure pulse and acoustic radiation from an oscillating piston. Compared to its counterpart in conservation form, the primitive variable nonlinear PML absorbing boundary condition shows no substantial difference in performance. However, significant improvements over the linear PML equations have been observed for strongly nonlinear problems.

Acknowledgments

This work is supported by Grants from 973 Program-2007CB714604, NSFC-50890181, NCET-07-0038 (X.D. Li and D.K. Lin) and NSF DMS-0810946 (F.Q. Hu). The authors also would like to thank the support from the 111 Project B07009 and B08009 of China.

References

- [1] Hu FQ. Absorbing boundary conditions. Int J Comput Fluid Dyn 2004;18(6): 513–22
- [2] Bodony DJ. Analysis of sponge zones for computational fluid mechanics. J Comput Phys 2006;212:681–702.
- [3] Hu FQ. Development of PML absorbing boundary conditions for computational aeroacustics: a progress review. Comput Fluids 2008;37:336–48.
- [4] Berenger JP. A perfectly matched layer for the absorption of electromagnetic waves. Comput Phys 1994;114:185–200.
- [5] Hu FQ. On absorbing boundary conditions for linearized Euler equations by a perfectly matched layer. | Comput Phys 1996;129:201–19.
- [6] Abarbanel S, Gottlieb D, Hesthaven JS. Well-posed perfectly matched layers for advective acoustics. J Comput Phys 1999;154:266–83.
- [7] Hu FQ. A stable perfectly matched layer for linearized Euler equations in unsplit physical variables. J Comput Phys 2001;173:455–80.
- [8] Bécache E, Fauqueux S, Joly P. Stability of perfectly matched layers, group velocities and anisotropic waves. J Comput Phys 2003;188:399–433.
- [9] Hagstrom T, Nazarov I. Perfectly matched layers and radiation boundary conditions for shear flow calculations. AIAA Paper 2003-3298; 2003.
- [10] Hu FQ, A perfectly matched layer absorbing boundary condition for linearized Euler equations with a non-uniform mean-flow. J Comput Phys 2005;208: 469–92.
- [11] Nataf F. A new approach to perfectly matched layers for the linearized Euler system. J Comput Phys 2006;214:757–72.
- [12] Hu FQ. On the construction of PML absorbing boundary condition for the nonlinear Euler equatins. AIAA Paper 2006-0798; 2006.
- [13] Hagstrom T, Goodrich J, Nazarov I, Dodson C. High-order methods and boundary.
- [14] Hagstrom T, Appelö D. Experiment with Hermite methods for simulating compressible flows: Runge-Kutta time-stepping and absorbing layers. AIAA Paper 2007-3505: 2007.
- [15] Hu FQ, Li XD, Lin DK. Absorbing boundary conditions for nonlinear Euler and Navier-Stokes equations based on the perfectly matched layer technique. J Comput Phys 2008;227:4398-424.
- [16] Parrish SA, Hu FQ. PML absorbing boundary conditions for the linearized and nonlinear Euler equations in the case of oblique mean flow. Int J Numer Meth Fluids 2009;60:565–89.
- [17] FQ. Hu, On perfectly matched layer as an absorbing boundary condition. AIAA Paper 96-1664; 1996.
- [18] Tam CKW, Webb JC. Dispersion-relation-preserving finite difference scheme for computational acoustics. J Comput Phys 1993;107:262–81.
- [19] Stanescu D, Habashi WG. 2N-storage low-dissipation and low-dispersion Runge-Kutta schemes for computational aeroacoustics. J Comput Phys 1998;143:674–81.
- [20] Bogey C, Cacqueray ND, Bailly C. A shock-capturing methodology based on adaptative spatial filtering for high-order non-linear computations. J Comput Phys 2009;228:1447–65.